Acta Mechanica 191, 21–35 (2007)
DOI 10.1007/s00707-007-0444-x
Printed in The Netherlands

Acta Mechanica

Influence of a magnetic field on natural convection in a shallow porous enclosure saturated with a binary fluid

D. S. Rakoto Ramambason and **P. Vasseur**, Montréal, Québec

Received June 28, 2006; revised September 18, 2006
Published online: April 16, 2007

Summary. An analytical and numerical investigation is conducted to study the effect of an electromagnetic field on natural convection in a horizontal shallow porous cavity filled with an electrically conducting binary mixture. A uniform heat flux is applied to the horizontal walls of the layer while the vertical walls are adiabatic. The solutal buoyancy forces are assumed to be induced either by the imposition of constant fluxes of mass on the horizontal boundaries (double diffusive convection) or by temperature gradients (Soret induced convection). Governing parameters of the problem under study are the thermal Rayleigh number, R_T, Hartmann number, Ha, Lewis number, Le, buoyancy ratio, φ, aspect ratio, A, and normalized porosity of the porous medium, ε. An analytical solution, valid for a shallow layer ($A \gg 1$) is derived on the basis of the parallel flow approximation. In the range of the governing parameters considered in this study, a good agreement is found between the analytical predictions and the numerical results obtained by solving the full governing equations.

Nomenclature

a	real number
A	aspect ratio of the cavity, L'/H'
$\vec{B}'_0$	applied magnetic field, volt.s.m^{-2}
C	dimensionless concentration
C_S	dimensionless concentration gradient in x-direction
C_T	dimensionless temperature gradient in x-direction
D	mass diffusivity of species, m^{2}s^{-1}
D'	thermal diffusion coefficient, m^{2}s^{-1}K^{-1}
g	gravitational acceleration, m s^{-2}
H'	height of layer, m
Ha	Hartmann number, $B'_0\sqrt{K\sigma/\mu}$
$\vec{J}'$	electric current density
j'	solute flux per unit area, kg m^{-2}s^{-1}
k	thermal conductivity, W m^{-1}K^{-1}
K	permeability of the porous medium, m^2
L'	layer width, m
Le	Lewis number, α/D
N	mass fraction

N_0 reference mass fraction
Nu Nusselt number, $1/\Delta T$
p' pressure
ΔN characteristic mass fraction difference
q' constant heat flux per unit area, W m^{-2}
R_T thermal Rayleigh number
R_T^* modified thermal Rayleigh number, $R_T/(1+Ha^2)$
S normalized mass fraction, $N/\Delta N$
Sh Sherwood number, $1/\Delta S$
t dimensionless time, $t'\alpha/H'^2$
T dimensionless temperature, $(T' - T'_0)/\Delta T'$
$\Delta T'$ characteristic temperature difference, $q'H'/k$
u dimensionless velocity in x-direction, $u'H'/\alpha$
v dimensionless velocity in y-direction, $v'H'/\alpha$
(x, y) Cartesian coordinates, $(x',y')/H'$

Greek symbols

α thermal diffusivity, m^2s^{-1}
β'_T thermal expansion coefficient, K^{-1}
β_N concentration expansion coefficient
φ buoyancy ratio, $\beta_N\Delta N/\beta'_T\Delta T'$
σ electrical conductivity, $ohm^{-1}m^{-1}$
μ dynamic viscosity of fluid, kg $m^{-1}s^{-1}$
ρ density of fluid, kg m^{-3}
$(\rho C)_f$ heat capacity of fluid, W K^{-1}
$(\rho C)_p$ heat capacity of saturated porous medium, W K^{-1}
γ heat capacity ratio, $(\rho C)_p/(\rho C)_f$
ψ dimensionless function, ψ'/α
ψ_0 dimensionless stream function at the center of the cavity
ϕ porosity of the porous medium
ε normalized porosity, ϕ/γ
Φ' electric potential

Subscript

.0. reference state

Superscript

′ refers to dimensional variable

1 Introduction

Coupled heat and mass transfer by natural convection in electrically conducting binary fluids saturated porous media, in the presence of a magnetic field, has attracted attention in recent years. This is due to the occurrence of such fluids in various engineering and geophysical applications.

Two types of problems, concerning natural convection of binary fluids in porous media, have been investigated so far. The first type of problem is the so-called double diffusive convection. For this situation, the solutal contribution to the total buoyancy force induced in the fluid mixture, by both the thermal and solutal gradients, results from given solutal boundary conditions applied on the walls of the cavity. A recent review of this topic has been presented by Mohamad et al. [1] and Boutana et al. [2]. The second type of problem is the Soret effect, also called thermal diffusion or thermodiffusion. This case corresponds to species migration induced, in an initial homogeneous mixture, by a thermal gradient. A recent paper by Bahloul et al. [3] presents a comprehensive account of the available information on this topic.

The effect of a magnetic field on the natural convection of a binary fluid in porous media has been considerably less investigated in the open literature despite its applications such as solidification of metal alloys, nuclear fuel debris removal, geothermal reservoirs, etc. Cheng [4] studied the effect of a magnetic field on double-diffusive convection over vertical plates embedded in electrically conducting fluid saturated porous media. This flow configuration was also considered by Hassanien and Obied Allah [5] to investigate the effect of permeability variation on oscillatory hydromagnetic flow through a porous medium in the presence of free convection and mass transfer flow. In a recent paper Postelnicu [6] has considered both Soret and Dufour effects on the natural convection about a vertical surface embedded in a saturated medium subjected to a magnetic field. The effects of the governing parameters on the heat and mass transfer are discussed. This flow configuration was also considered by Takhar et al. [7] for the case of a porous plate moving with time dependent velocity in an ambient fluid. The effects of both a magnetic field and Hall current on the velocity profiles have been predicted numerically. Recently, the problem of simultaneous heat and mass fluxes, around a permeable sphere maintained at uniform heat and mass fluxes, in the presence of a magnetic field and thermal radiation effects has been investigated by Chamkha and Al-Mudhaf [8]. It was found that both Nusselt and Sherwood numbers decreased due to increases in either the Hartmann number or the circumferential position.

In this paper the influence of a magnetic field on convection of a binary fluid saturating a horizontal shallow porous cavity is considered. The cavity is heated from the bottom and cooled from the top by constant heat fluxes. Both double-diffusive convection and Soret-induced convection are considered. An analytical solution, valid in the limit of a shallow cavity ($A \gg 1$) is derived on the basis of the parallel flow approximation. Numerical confirmation of the stable analytical results is also presented.

2 Mathematical formulation

The flow configuration under study is shown in Fig. 1. It consists of a two dimensional shallow enclosure of thickness H', width L', permeability K and porosity ϕ filled with an electrically conducting binary fluid. A uniform and constant magnetic field $\vec{B'}_0$ is applied parallel to gravity. The magnetic Reynolds number is assumed to be small so that the induced magnetic field can be neglected in comparison with the applied magnetic field. Also the Hall effect is assumed to be

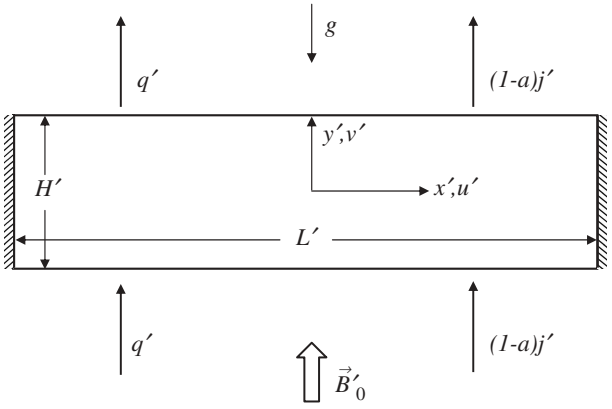

Fig. 1. Schematic of the problem

negligible. The mixture is assumed to satisfy the Boussinesq approximation. Thus, the density variation with temperature and concentration is described by the state equation

$$\rho = \rho_0\left[1 - \beta'_T\left(T' - T'_0\right) - \beta_N(N - N_0)\right] \tag{1}$$

where ρ_0 is the fluid mixture density at temperature $T' = T'_0$ and mass fraction $N = N_0$, and β'_T and β_N are the thermal and concentration expansion coefficients, respectively. The subscript 0 refers to the condition at the origin of the coordinate system.

The mass fraction of the denser component of the mixture, N_0, is assumed to be initially uniform. According to De Groot and Mazur [9] the expressions relating the thermal and solute gradients present in a binary fluid mixture are given by

$$Q' = -k\nabla T' \tag{2}$$

and

$$J'(1-a) = -\rho D\nabla N - a\rho D'N(1-N)\nabla T', \tag{3}$$

where k and D are the thermal conductivity and the mass diffusivity of species through the fluid-saturated porous medium, D' is the effect of thermal diffusion coefficient and a is a real number, the significance of which will be discussed below.

The equations governing the conservation of mass, momentum, energy, species and electric charge transfer for laminar flows are written as follows:

$$\nabla \cdot \vec{V'} = 0, \tag{4}$$

$$\frac{\mu}{K}\vec{V'} = -\nabla p' + \rho\vec{g} + \vec{J'} \times \vec{B}'_0, \tag{5}$$

$$(\rho C)_p \frac{\partial T'}{\partial t'} + (\rho C)_f(\vec{V'}.\nabla T') = k\nabla^2 T', \tag{6}$$

$$\phi\frac{\partial N}{\partial t'} + \vec{V'}.\nabla N = D\nabla^2 N + D'N(1-N)\nabla^2 T', \tag{7}$$

$$\nabla.\vec{J'} = 0;\ \vec{J'} = \sigma\left(-\nabla\Phi' + \vec{V'} \times \vec{B}'_0\right), \tag{8}$$

where $\vec{V'}$ is the Darcy velocity, $\vec{g}$ the gravitational acceleration, ϕ the porosity of the porous medium, μ the kinematic viscosity, and $(\rho C)_f$ and $(\rho C)_p$ are respectively the heat capacity of the fluid and the saturated porous medium.

In Eq. (8) $\vec{J'}$ is the electric current density, σ the electrical conductivity, Φ' the electric potential and $-\nabla\Phi'$ the associated electric field. As discussed by Garandet et al. [10], for a two-dimensional situation Eq. (8) for the electric potential reduces to $\nabla^2\Phi' = 0$. The unique solution is $\nabla\Phi' = 0$ since there is always an electrically insulating boundary around the enclosure on which $\partial\Phi/\partial n = 0$. It follows that the electric field vanishes everywhere. In the absence of an electric field, the small magnetic Reynolds number assumption uncouples Maxwell equations from the momentum equation [11]. The Lorentz force then reduces to a systematically damping factor.

The boundary conditions applied on the horizontal boundaries of the system are uniform fluxes of heat and mass per unit area, q' and $(1-a)j'$, respectively. All boundaries are assumed to be impermeable. The case $a = 0$ corresponds to double-diffusive convection for which the solutal buoyancy forces in the porous layer are induced by the external imposition of a constant mass flux boundary condition j'. The case $a = 1$ corresponds to the case of a binary mixture subject to the Soret effect (no externally imposed mass flux). Thus when $a = 0$, Eq. (3) is the usual mass flux, while for $a = 1$ the right hand side term represents the Soret effect, i.e. the contribution of temperature gradient to the mass flux.

The dimensionless variables (primed quantities are dimensional) are introduced as follows:

$$(x, y) = (x', y')/H', \quad (u, v) = (u', v')H'/\alpha, \tag{9}$$

$$t = t'\alpha/H'^2, \quad \varepsilon = \phi/\gamma,$$

$$T = \left(T' - T'_0\right)/\Delta T', \quad \Delta T' = q'H'/k,$$

$$\psi = \psi'/\alpha, \quad S = N/\Delta N,$$

where $\gamma = (\rho C)_p/(\rho C)_f$ is the heat capacity ratio and $\Delta N = -j'/\rho D$ for double-diffusive convection while $\Delta N = N_0(1-N_0)\Delta T' D'/D$ for Soret-driven convection.

It is assumed here that the Soret effect is small such that $N(1-N)$ can be approximated by $N_0(1-N_0)$ (see for instance [12]). Eliminating the pressure term in Eq. (5) in the usual way and with the definitions in Eq. (9), it is readily shown that the dimensionless governing equations can be expressed as follows:

$$\nabla^2\psi = -R_T\left(\frac{\partial T}{\partial x} + \varphi\frac{\partial S}{\partial x}\right) - Ha^2\frac{\partial^2\psi}{\partial y^2}, \tag{10}$$

$$\frac{\partial T}{\partial t} + u\frac{\partial T}{\partial x} + v\frac{\partial T}{\partial y} = \nabla^2 T, \tag{11}$$

$$\varepsilon\frac{\partial S}{\partial t} + u\frac{\partial S}{\partial x} + v\frac{\partial S}{\partial y} = \frac{1}{Le}\left(\nabla^2 S - a\nabla^2 T\right), \tag{12}$$

where ψ is the usual dimensionless stream function defined as $u = \partial\psi/\partial y$ and $v = -\partial\psi/\partial x$. The term on the right-hand side of Eq. (10) includes the Lorentz force induced by the interaction of the magnetic field with convective motion (see for instance [10], [13]–[15]).

The non-dimensional boundary conditions over the walls of the enclosure are as follows:

$$x = \pm A/2, \quad \psi = 0, \quad \frac{\partial T}{\partial x} = \frac{\partial S}{\partial x} = 0, \tag{13}$$

$$y = \pm 1/2, \quad \psi = 0, \quad \frac{\partial T}{\partial y} = -1, \quad \frac{\partial S}{\partial y} = (a-1) + a\frac{\partial T}{\partial y}.$$

Equations (10)–(12) together with the boundary conditions, Eqs. (13), complete the formulation of the problem. The dimensional groups appearing after the nondimensionalization process are the thermal Rayleigh number R_T, buoyancy ratio φ, Lewis number Le , Hartmann number Ha , aspect ratio of the cavity A, normalized porosity ε and constant a. These parameters are given by

$$R_T = \frac{gKH'\beta'_T\Delta T'}{\alpha\nu}, \quad Le = \frac{\alpha}{D}, \quad \varphi = \frac{\beta_N \Delta N}{\beta'_T \Delta T'}, \tag{14}$$

$$Ha = B'_0\left(\frac{K\sigma}{\mu}\right)^{1/2}, \quad A = L'/H', \quad \varepsilon = \phi/\gamma,$$

where μ is the dynamic viscosity of the mixture and γ the electrical conductivity.

In the present study the heat and solute transports are expressed in terms of the Nusselt and Sherwood numbers defined respectively as

$$Nu = \frac{1}{\Delta T}, \quad Sh = \frac{1}{\Delta S}, \tag{15}$$

where $\Delta T = T(0,-1/2) - T(0,1/2)$ and $\Delta S = S(0,-1/2) - S(0,1/2)$ are the temperature and concentration differences, evaluated at $x = 0$.

3 Numerical solution

The solution of the governing equations and boundary conditions, Eqs. (10)–(13), is obtained using a control volume approach and the SIMPLER algorithm [16]. A finite difference procedure with variable grid is considered for better consideration of the boundary conditions. The power-law scheme is used to evaluate the flow, heat and mass fluxes across each of the control volume boundaries. A second order backwards finite difference scheme is employed to discretize the temporal terms appearing in the governing equations. The discretized momentum, energy and concentration equations are underrelaxed to accelerate the convergence. The relaxation parameter was chosen equal to 0.5. A Thomas iterative procedure is employed to solve the resulting discretized equations. At each new time step, the updating of the physical new variables is done until the convergence criterion $\sum_{i=1}^{m}(b_i^k - b_i^{k-1}) \Big/ \sum_{i=1}^{m} b_i^k \leq 10^{-9}$ is satisfied, where b stands for ψ, T and S.

The effects of the strength of the magnetic field on Soret driven convection ($a = 1$) within a square enclosure ($A = 1$) are illustrated in Figs. 2a–c for $R_T = 250$, $Le = 10$ and $\varphi = 0.5$. The results are presented in terms of streamlines (on the left), isotherms (at the center) and iso-concentration (on the right) contours for different values of Ha. The flow directions in the graphs can be easily identified according to the distributions of temperature and solute. The intervals of streamlines, isothermal and iso-concentration lines are $\Delta\phi = (\phi_{\max} - \phi_{\min})/11$, where ϕ stands for ψ, T and S.

Figure 2a shows the results obtained for $Ha = 0$, i.e., in the absence of a magnetic field. This situation corresponds to a classical Bénard situation for which the supercritical Rayleigh number $R_{TC}^{\sup}$ for the onset of convection is given by $R_{TC}^{\sup} = 22.95/[1 + \varphi(Le + a)]$ as predicted by Bahloul, Boutana and Vasseur [3] and Mamou and Vasseur [17], Eq. (28) with $R^{sup} = 22.95$ when $A = 1$. For the situation considered here $R_{TC}^{sup} = 3.53$, and this analytical prediction has been checked numerically with the present code. Above this critical value convection occurs and the flow field consists of a single cell. The direction of the fluid circulation, which can be

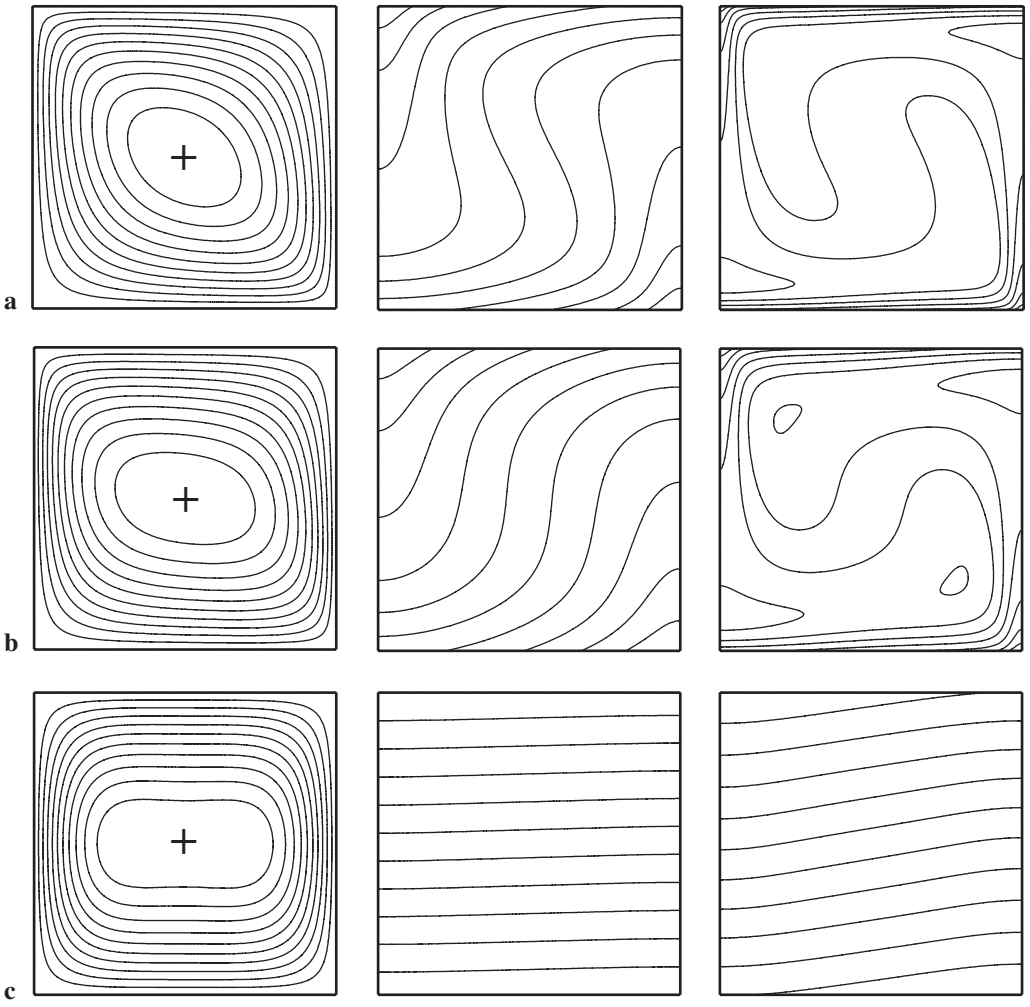

Fig. 2. Stream function, temperature and concentration lines for $R_T = 250$, $Le = 10$, $\varphi = 0.5$, $A = 1$, $a = 1$: **a** $Ha = 0$, $\psi_0 = 5.151$, $Nu = 4.366$, $Sh = 16.703$; **b** $Ha = 2$, $\psi_0 = 2.584$, $Nu = 2.597$, $Sh = 12.422$; **c** $Ha = 10$, $\psi_0 = 0.381$, $Nu = 1.001$, $Sh = 1.017$

either clockwise or counterclockwise, is induced by the round-off errors generated in the numerical computation. Owing to the values of the governing parameters considered here, the resulting convection is relatively large, as indicated by the value of the stream function at the center of the cavity $\psi_0 = 5.151$ and the large distortion of the temperature and concentration fields ($Nu = 4.366$ and $Sh = 16.703$). The retarding effects of magnetic drag on the flow pattern of Fig. 2a are demonstrated in Figs. 2b and c, for $Ha = 2$ and 10, respectively. The results indicate that, for given values of R_T, A, Le and φ, the convective circulation is progressively inhibited as the value of Ha is increased. Thus when $Ha = 2$, Fig. 2b shows that the overall strength of the circulation is considerably reduced ($\psi_0 = 2.584$) in comparison to that of Fig. 2a. In fact, for $Ha = 10$, Fig. 2c indicates that the convective motion within the cavity is almost completely damped ($\psi_0 = 0.381$) by the magnetic drag. As a result the heat ($Nu = 1.001$) and mass ($Sh = 1.017$) transfer are almost purely conductive, as indicated by the nearly horizontal isotherms and isoconcentrations.

Figures 3a and b illustrate the numerical results obtained for $R_T = 200$, $Le = 10$, $\varphi = 0$, $A = 8$, $Ha = 1$ and $a = 0$ (double-diffusive convection) and $a = 1$ (Soret-driven convection). The results clearly illustrate the fact that for a shallow cavity ($A \gg 1$) the flow in the core region of the enclosure is essentially parallel while the temperature and concentration in the core are linearly stratified in the horizontal direction. The analytical solution, developed in the following Section, relies on these observations.

In the present problem, numerical tests have been performed to determine the minimum aspect ratio above which the flow can be assumed parallel. Typical results are presented in Fig. 4 for the case $R_T = 200$, $Le = 1$, $\varphi = 0$, $a = 0$ and $Ha = 0$ and 1. It is found that, as the value of A is made sufficiently large, ψ_0 and Nu (or Sh) tend asymptotically toward constant values predicted by the analytical solution discussed in the following Section. In general, it was found that the numerical results can be considered independent of the aspect ratio when $A \gg 8$. For this reason, most of the results reported in this study were obtained for $A = 10$, with typically 60×180 mesh points.

4 Analytical solution

In the limit of a shallow cavity it is possible to find an approximate analytical solution to the set of equations (10)–(12) subject to boundary conditions (13). The procedure is similar to that

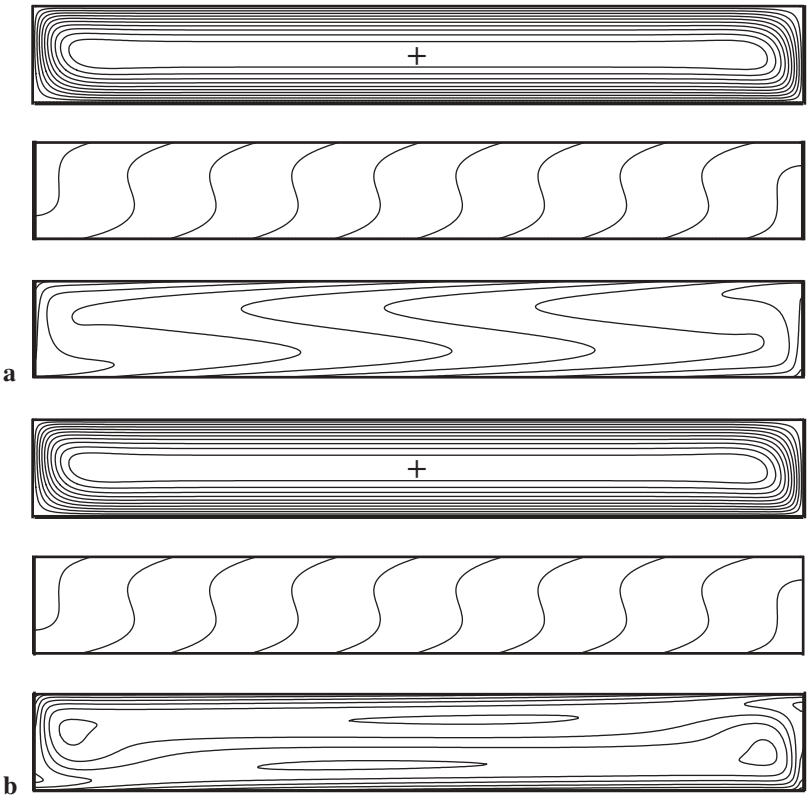

Fig. 3. Stream function, temperature and concentration lines for $R_T = 200$, $Le = 10$, $\varphi = 0$, $A = 8$, $Ha = 1$: **a** $a = 0$, $\psi_0 = 3.706$, $Nu = 3.734$, $Sh = 6.059$; **b** $a = 1$, $\psi_0 = 3.706$, $Nu = 3.734$, $Sh = 6.511$

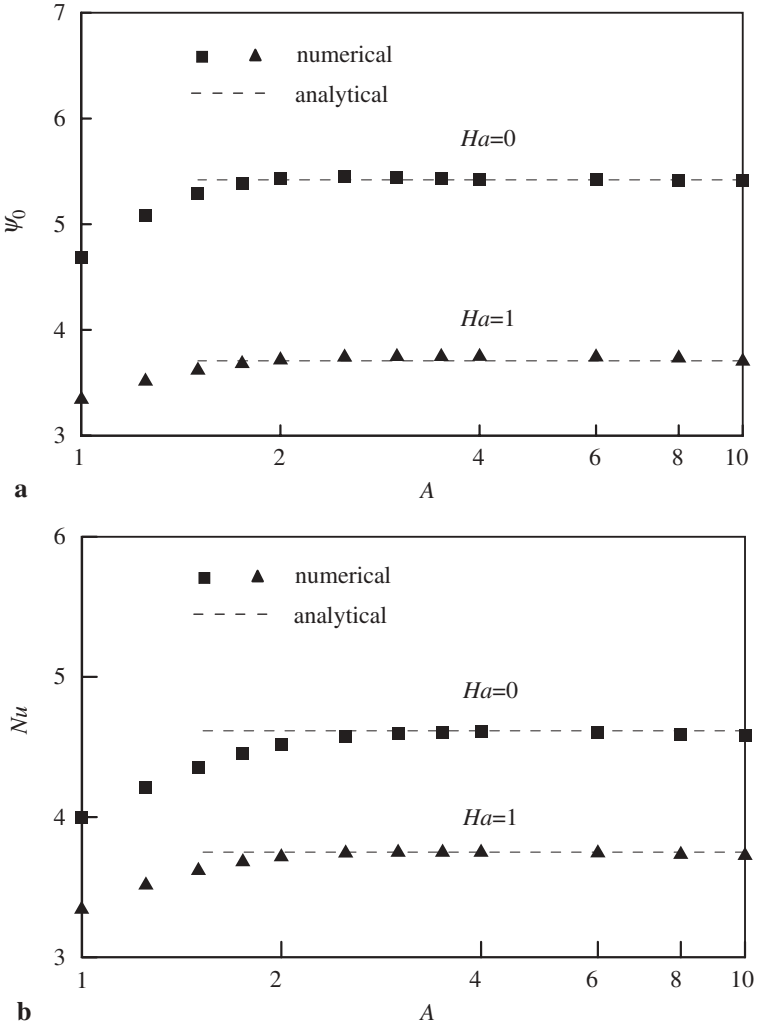

Fig. 4. Effect of aspect ratio A and Nu for $R_T = 200$, $Le = 1$, $\varphi = 0$, $a = 0$ and $Ha = 0$ and 1

given by Bahloul et al. [3] such that only the final results are presented here. Thus, for the present problem, it is found that the stream function and the temperature and concentration fields are given by:

$$\psi(y) = \psi_0\left(1 - 4y^2\right), \tag{16}$$

$$T = C_T x + \frac{\psi_0}{3} C_T\left(3y - y^3\right) - y, \tag{17}$$

$$S = C_S x + \frac{\psi_0}{3}\left(LeC_S + aC_T\right)\left(3y - 4y^3\right) - y. \tag{18}$$

In the above equations C_T and C_S are given by:

$$C_T = \frac{4b\psi_0}{3\left(2b + \psi_0^2\right)}, \tag{19}$$

$$C_S = \frac{-3aC_T\left(Le\psi_0^2 - 2b\right) + 4bLe\psi_0}{3\left(2b + \psi_0^2 Le^2\right)}, \tag{20}$$

where $b = 15/16$ and ψ_0, the value of the stream function at the center of the cavity, can be evaluated from the following expressions:

$$\psi_0 = \pm\frac{\sqrt{b}}{Le}\left[d_1 \pm \sqrt{d_1^2 + d_2}\right]^{1/2}, \tag{21}$$

where

$$d_1 = \frac{R_T^* Le}{12}[Le + \varphi(1-a)] - \left(Le^2 + 1\right), \tag{22}$$

$$d_2 = \frac{R_T^* Le^2}{3}[1 + \varphi(Le + a)] - 4Le^2, \tag{23}$$

$$R_T^* = \frac{R_T}{(1 + Ha^2)}. \tag{24}$$

It is noted that $\psi_0 = 0$, i.e. the rest state, is also a solution predicted by the present analysis. The transition from the rest state ($\psi_0 = 0$) to convection ($\psi_0 \neq 0$) will be discussed later on.

The local heat and mass transfer rates are given, according to Eqs. (17), (18) and (15), by

$$Nu = \frac{6\left(\psi_0^2 + 2b\right)}{\psi_0^2 + 12b}, \tag{25}$$

$$Sh = \frac{Sh_0}{1 + Sh_0(Nu - 1)/Nu}, \tag{26}$$

where

$$Sh_0 = \frac{6\left(\psi_0^2 Le^2 + 2b\right)}{\psi_0^2 Le^2 + 12b}. \tag{27}$$

Figures 5a–c exemplify the bifurcation diagrams in terms of ψ_0, Nu and Sh versus R_T for the case $Le = 10$, $a = 1$ (Soret-induced convection) and various values of Ha. The curves depicted in these graphs are the predictions of the parallel flow approximation. The numerical solution of the full governing equations, depicted by dots, is seen to be in good agreement with the analytical solution. The results are obtained for $\varphi > 0$, namely $\varphi = 0.5$, for which the thermal and solutal buoyancy forces are destabilizing. For this situation the onset of convection from the rest state ($\psi_0 = 0$) to convection ($\psi_0 \neq 0$) occurs through a supercritical Rayleigh number $R_{TC}^{\sup}$. This threshold is predicted by the present theory from the conditions $d_1 < 0$ and $d_2 = 0$ such that Eqs. (21)–(23) yield the following critical value:

$$R_{TC}^{\sup} = \frac{R^{\sup}(1 + Ha^2)}{[1 + \varphi(Le + a)]}, \tag{28}$$

where $R^{\sup} = 12$.

In the absence of a magnetic field ($Ha = 0$) the onset of supercritical Rayleigh number $R_{TC}^{\sup}$ occurs at a supercritical Rayleigh number $R_{TC}^{\sup} = 1.846$, Eq. (28), and the resulting pitchfork bifurcation curves are similar to those reported in the literature (see for instance Bahloul et al. [3]). As the magnetic field, i.e., Ha , is increased, Figs. 5a–c indicate that onset of motion occurs at a larger supercritical Rayleigh number. Thus, for instance, $R_{TC}^{\sup} = 9.231$ for $Ha = 2$ and $R_{TC}^{\sup} = 48$ for $Ha = 5$. Also, Fig. 5a indicates that, for a given Rayleigh number R_T, the flow

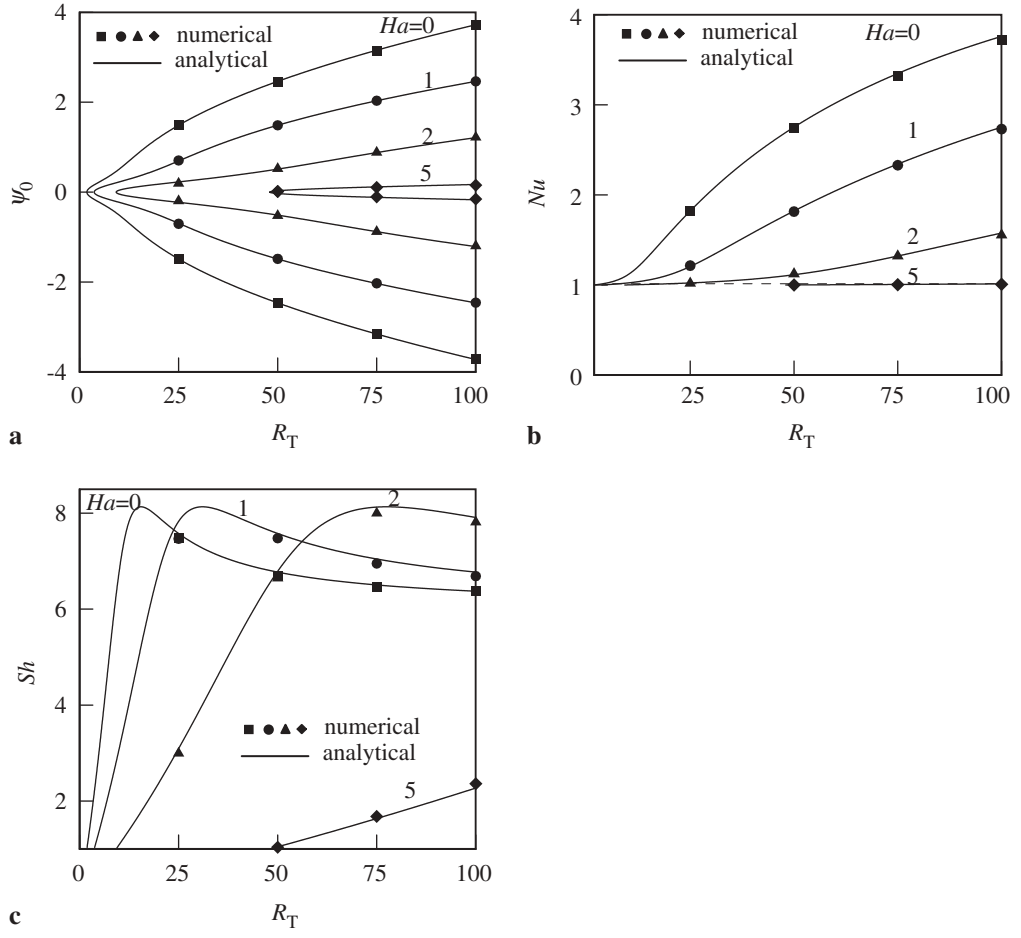

Fig. 5. Bifurcation diagram in terms of **a** ψ_0, **b** Nu, **c** Sh, versus R_T for $\varphi = 0.5$, $Le = 10$, $a = 1$ and various values of Ha

circulation is considerably inhibited by the retarding effect of the electromagnetic body force. As a result Fig. 5b shows that the Nusselt number Nu decreases considerably with Ha. Hence, for $Ha = 5$, it is found that the heat transfer is almost by pure conduction ($Nu \approx 1$) for the range of the Rayleigh number considered here. The effect of Ha on the Sherwood number, depicted in Fig. 5c, is observed to be less straightforward. This is due to the fact that Sh, for Soret induced convection ($a = 1$), has not it usual significance. For this situation, it is assumed that the walls of the cavity are impermeable such that $J' = 0$ (Eq. (3)). As a result Sh is rather related to the concentration distribution within the cavity induced by the Soret effect and by convection.

Figures 6a–c show the results obtained for the same conditions of Figs. 5a–c but for $\varphi < 0$, namely $\varphi = -0.5$. For this situation, for which the thermal and solutal forces are opposing each other, it is well known (see [17] for instance), that under appropriate conditions convection takes place through a subcritical bifurcation. The onset of convection occurs with a finite amplitude convection of magnitude $\psi_0 = \pm\sqrt{bd_1}/Le$. The subcritical Rayleigh number R_{TC}^{sub} for the onset of convection is obtained from the conditions $d_1 > 0$ and $d_1^2 + d_2 = 0$ as

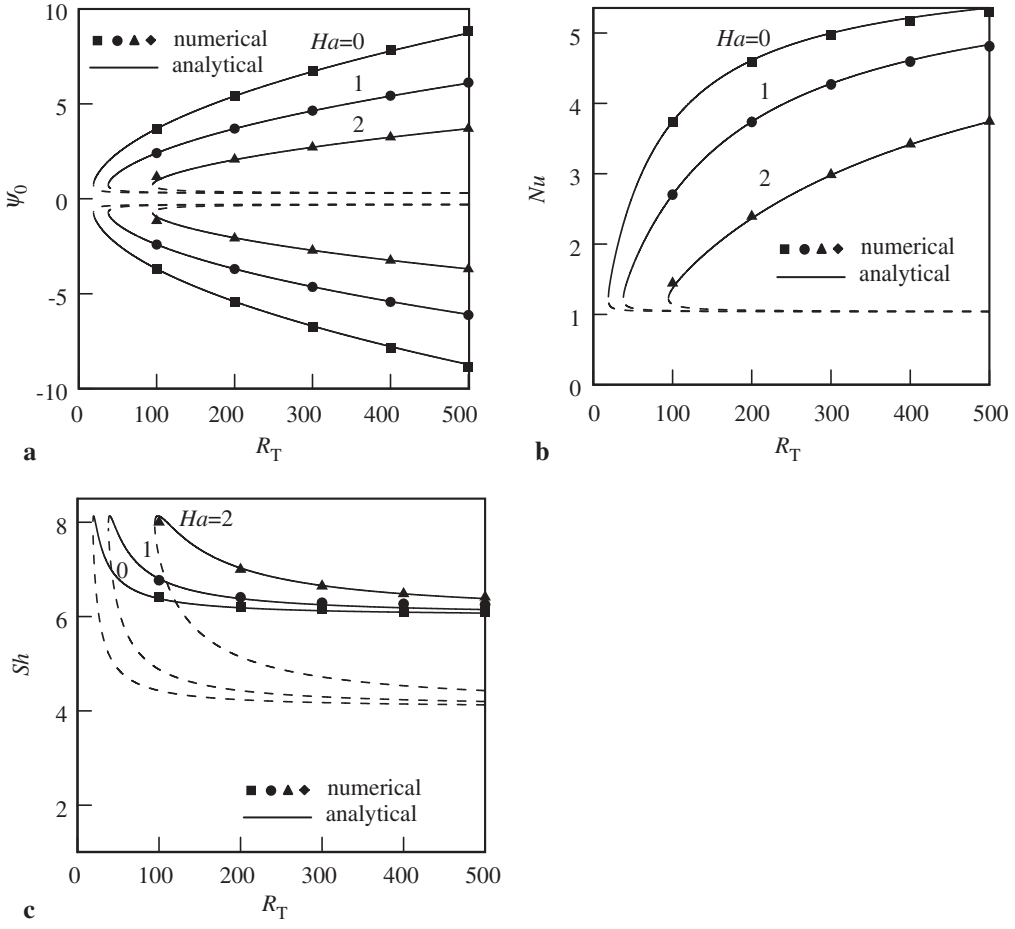

Fig. 6. Bifurcation diagram in terms of **a** ψ_0, **b** Nu, **c** Sh, versus R_T for $\varphi = -0.5$, $Le = 10$, $a = 1$ and various values of Ha

$$R_{TC}^{sub} = \frac{(1+Le)R^{\sup}(1+Ha^2)}{Le[Le+\varphi(1-a)]^2}[(Le-1)(Le-\varphi) - a\varphi(Le+1) + 2\sqrt{\varphi Le(Le+a-1)(a\varphi - Le+1)}]. \quad (29)$$

For the conditions considered in the graphs the subcritical Rayleigh numbers for the onset of convection are $R_{TC}^{sub} = 18.954$ for $Ha = 0$, $R_{TC}^{sub} = 37.910$ for $Ha = 1$ and $R_{TC}^{sub} = 94.769$ for $Ha = 2$.

Another view of the effect of the Hartmann number Ha on the present problem is illustrated in Figs. 7a and b for the case $Le = 2$ and $a = 0$ and 1. The case of pure thermal convection ($\varphi = 0, a = 0$), presented for comparison purpose, corresponds to a classical Bénard situation. It gives rise to a supercritical Rayleigh number $R_{TC}^{\sup} = 12$, as predicted by Nield [18]. The way that this pitchfork bifurcation is affected by the solutal buoyancy forces is presented in Fig. 7a for $\varphi = 0.2$ for which the thermal and solutal forces are destabilizing. The results show that pitchfork bifurcations are obtained at $R_{TC} = 8.571$ for double-diffusive convection ($a = 0$) and $R_{TC} = 7.500$ for Soret-induced convection ($a = 1$). The results obtained for $\varphi = -0.2$ are presented in Fig. 7b. For this situation, for which the thermal and solutal forces are opposing

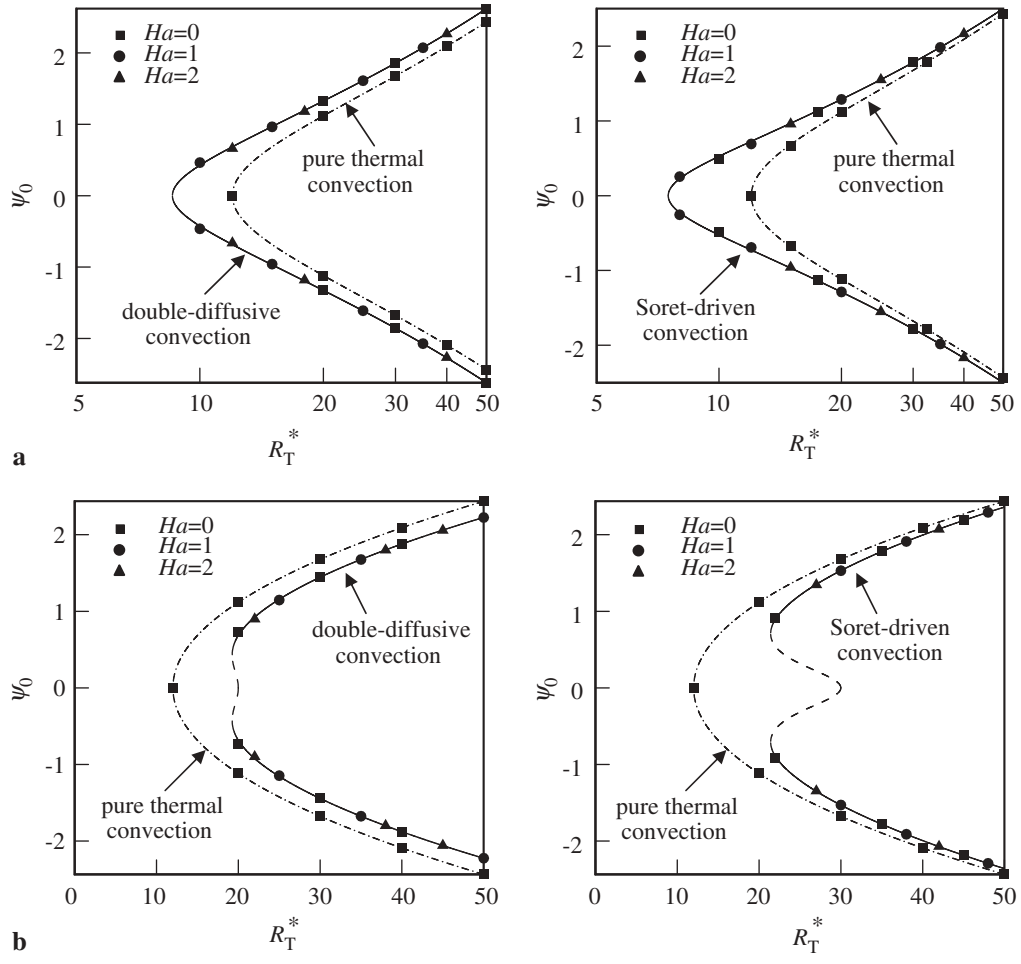

Fig. 7. Bifurcation diagram in terms of ψ_0 versus R_T^* for $Le = 2$, $a = 0{,}1$ and **a** $\varphi = 0.2$, **b** $\varphi = -0.2$

each other, the graph indicates the occurrence of subcritical bifurcation as already discussed. For the conditions considered here $R_{TC}^{sub} = 19.249$ for $a = 0$ and $R_{TC}^{sub} = 21.418$ for $a = 1$.

It is clear from Eqs. (21)–(27), that all the curves at different Hartmann numbers, as presented in Figs. 5 and 6 for instance, collapse in single curves with the use of a modified Rayleigh number $R_T^* = R_T/(1 + Ha^2)$. This point, confirmed by the numerical solution of the full governing equations obtained for various values of Ha, is valid only in the limit of a shallow cavity ($A \gg 1$).

5 Conclusions

In this paper we have examined the effect of a vertical transverse magnetic field on natural convection, of an electrically conducting binary fluid saturated porous medium, confined in a shallow horizontal cavity. The case of double-diffusion convection ($a = 0$) is compared with the case of Soret-driven convection ($a = 1$). The governing equations for the porous medium,

modeled according to Darcy's model, have been solved using a combination of analytical and numerical techniques. The governing parameters of the problem are the thermal Rayleigh number R_T, buoyancy ratio φ, Lewis number Le, normalized porosity of the porous medium ε, Hartmann number Ha, aspect ratio of the layer A, and the type of convection (i.e., parameter a) considered. Detailed results for the flow field and heat and mass transfer rates have been presented for comparison. From these results, the following remarks are in order:

(i) Under the condition of constant heat and mass fluxes imposed on the horizontal walls of the layer the flow structure in a shallow cavity ($A \gg 1$), in the absence of a magnetic field ($Ha = 0$), is parallel in the core of the cavity. This flow structure is not affected by the imposition of a magnetic field.

(ii) An analytical solution, based on the parallel flow approximation, has been derived for the case of a shallow cavity ($A \gg 1$). The resulting nonlinear model yields the supercritical Rayleigh number $R_{TC}^{\sup}$ and subcritical Rayleigh number R_{TC}^{sub} for the onset of convection. For finite-amplitude convection, useful expressions have been obtained for velocity, temperature and solute distributions in the core of the layer. It is demonstrated that the retarding effect of the electromagnetic body Lorentz force decreases the strength of the convective motion within the layer and thus the convective heat and mass transfers.

(iii) The main features of the approximate theoretical solution have been tested by a numerical solution of the full governing equations.

References

[1] Mohamad, A. A., Bennacer, R., Azaiez, J.: Double diffusion natural convection in a rectangular enclosure filled with binary fluid saturated porous media: the effect of lateral aspect ratio. Phys. Fluids **16**, 184–199 (2004).

[2] Boutana, N., Bahloul, A., Vasseur, P., Joly, F.: Soret-driven and double-diffusive natural convection in a vertical porous cavity. J. Porous Media **7**, 1–17 (2004).

[3] Bahloul, A., Boutana, N., Vasseur, P.: Double-diffusive and Soret-induced convection in a shallow horizontal porous layer. J. Fluid Mech. **491**, 325–352 (2003).

[4] Cheng, C.-Y.: Effect of a magnetic field on heat and mass transfer by natural convection from vertical surfaces in porous media- an integral approach. Int. Comm. Heat Mass Transf. **26**, 935–943 (1999).

[5] Hassanien, I. A., Obied Allah, M. H.: Oscillatory hydromagnetic flow through a porous medium with variable permeability in the presence of free convection and mass transfer flow. Int. Commun. Heat Mass Transf. **29**, 567–575 (2002).

[6] Postelnicu, A.: Influence of a magnetic field on heat and mass transfer by natural convection from vertical surfaces in porous media considering Soret and Dufour effects. Int. J. Heat Mass Transf. **47**, 1467–1472 (2004).

[7] Takhar, H. S., Roy, S., Nath, G.: Unsteady free convection flow over an infinite vertical porous plate due to the combined effects of thermal and mass diffusion, magnetic field and Hall currents. Heat Mass Transf. **39**, 825–834 (2003).

[8] Chamkha, A. J., Al-Mudhaf, A.: Simultaneous heat and mass transfer from a permeable sphere at uniform heat and mass fluxes with magnetic field and radiation effects. Numer. Heat Transf. **46**, 181–198 (2004).

[9] De Groot, S. R., Mazur, P.: Non equilibrium thermodynamics. Amsterdam: North-Holland Pub. Co. 1969.

[10] Garandet, J. P., Alboussiere, T., Moreau, R.: Buoyancy-driven convection in a rectangular enclosure with a transverse magnetic field. Int. J. Heat Mass Transf. **35**, 741–748 (1992).

[11] Cramer, K. R., Pai, S. I.: Magneto fluid dynamics for engineers and applied physicists. New York: McGraw Hill 1973.

[12] Bergeron, A., Henry, D., Benhadid, H.: Marangoni-Bénard instability in microgravity conditions with Soret effect. Int. J. Heat Mass Transf. **37**, 1545–1562 (1994).
[13] Cheng, C. Y.: An integral approach for hydromagnetic natural convection heat and mass transfer from vertical surfaces with power-law variation in wall temperature and concentration in porous media. Int. Commun. Heat Mass Transf. **32**, 204–213 (2005).
[14] Postelnicu, A.: Influence of a magnetic field on heat and mass transfer by natural convection from vertical surfaces in porous media considering Soret and Dufour effects. Int. J. Heat Mass Transf. **47**, 1467–1472 (2004).
[15] Chamkha, A. J., Al-Naser, H.: Hydromagnetic double-diffusive convection in a rectangular enclosure with uniform side heat and mass fluxes and opposing temperature and concentration gradients. Int. J. Thermal Sci. **41**, 936–948 (2002).
[16] Patankar, S. V.: Numerical heat transfer and fluid flow. Washington: Hemisphere Pub. Corp. 1980.
[17] Mamou, M., Vasseur, P.: Thermosolutal bifurcation phenomena in porous enclosures subject to vertical temperature and concentration gradients. J. Fluid Mech. **395**, 61–87 (1999).
[18] Nield, D. A.: Onset of thermohaline convection in porous medium. Water Res. Res. **4**, 553–560 (1968).

Authors' address: D. S. Rakoto Ramambason and P. Vasseur, Mechanical Engineering Departement, Ecole Polytechnique de Montréal, Montréal, Québec, H3C3A7, Canada (E-mail: patrick.vasseur@polmtl.ca)